Fusogenic supramolecular vesicle systems induced by metal ion binding to amphiphilic ligands

Antoine Richard*, Valérie Marchi-Artzner*†, Marie-Noëlle Lalloz‡, Marie-Josèphe Brienne*, Franck Artzner§, Thaddée Gulik-Krzywicki¶, Marie-Alice Guedeau-Boudeville‖, and Jean-Marie Lehn*‡*

*Laboratoire de Chimie des Interactions Moléculaires and ‖Laboratoire de Physique de la Matière Condensée, Collège de France, 11 Place Marcelin Berthelot, 75231 Paris Cedex 05, France; ‡Institut de Science et d'Ingénierie Supramoléculaires, 8 Allée Gaspard Monge, BP 70028, 67083 Strasbourg Cedex, France; §Laboratoire de Physique de la Matière Condensée, Unité Mixte de Recherche 6626, Université de Rennes 1, 35064 Rennes Cedex, France; and ¶Centre de Génétique Moléculaire, Avenue de la Terrasse, 91198 Gif-sur-Yvette Cedex, France

Contributed by Jean-Marie Lehn, September 8, 2004

The incorporation of lipophilic ligands into the bilayer membrane of vesicles offers the possibility to induce, upon binding of suitable metal ions, a variety of processes, in particular vesicle aggregation and fusion and generation of vesicle arrays, under the control of specific metal–ligand recognition events. Synthetic bipyridine lipoligands Bn bearing a bipyridine unit as head group were prepared and incorporated into large unilamellar vesicles. The addition of Ni^{2+} or Co^{2+} metal ions led to the formation of complexes MBn and MBn_2 followed by spontaneous fusion to generate giant multilamellar vesicles. The metal ion complexation was followed by UV spectroscopy and the progressive fusion could be visualized by optical dark-field and fluorescence microscopies. Vesicle fusion occurred without leakage of the aqueous compartments and resulted in the formation of multilamellar giant vesicles because of the stacking of the lipoligands Bn. The fusion process required a long enough oligoethylene glycol spacer and a minimal concentration of lipoligand within the vesicle membrane. Metallosupramolecular systems such as the present one offer an attractive way to induce selective intervesicular processes, such as vesicle fusion, under the control of molecular recognition between specific metal ions and lipoligands incorporated in the bilayer membrane. They provide an approach to the design of artificial "tissue-mimetics" through the generation of polyvesicular arrays of defined architecture and to the control of their functional properties.

vesicle fusion | molecular recognition

In biological systems, ion binding or Ca^{2+} influx acts as a first signal driving membrane events such as fusion of secretory vesicles or cell membranes, or discharge of vesicle contents (1). Molecular recognition processes provide a powerful tool to induce selective interaction at the interface of vesicular membranes that may result in aggregation, adhesion, and fusion. The development of chemical liposomal systems undergoing such events provides approaches to mimicking biomembrane and biological cellular processes (2–5). It leads as well to the design of artificial bilayer vesicles presenting a range of novel properties and applications [for instance in materials science (6)]. It may extend from single vesicle features to the complex behavior of multivesicular arrays aimed at building artificial entities of "tissue-mimetic" nature that might undergo "physiological" type functions (e.g., signalization, network operation, and coupling and feedback between multiple reactions and compartments). Such developments are of particular interest as vesicle compartmentalization, self-organization, and functional integration represent steps toward more and more complex states of matter (7).

Molecular recognition between amphiphiles bearing complementary hydrogen-bonding groups (5), such as nucleobase (8–12) or oligonucleotide (13–15) derivatives, has been used to induce selective intervesicular and vesicle–layer interactions. In our group, we have investigated vesicles decorated with multiple hydrogen-bonding recognition groups, recosomes (16), that undergo selective interaction and fusion events (17–20). The coordination of specific metal ions with suitably designed ligands, i.e., metal-ion recognition events, may be implemented to similar ends. It has been extensively used for the self-assembly of a great variety of metallosupramolecular architectures (21–24). On the other hand, metallolipids such as annelides (25) have been shown to form metallomicelles (25, 26).

Lipidic derivatives of ligands, lipoligands, may serve as membrane additives making bilayer vesicles susceptible to undergoing processes induced by metal-ion binding. Thus, metal–ligand interaction could be used as a chemical reversible connector to self-organize objects that are themselves self-organized. The complexation of ions at the interface of vesicles decorated with amphiphilic synthetic ligands offers means to build up vesicle arrays of tissue-like character. Two different processes may be considered, depending on the location of the complex on the same vesicle (intravesicular complex) or between two different vesicles (intervesicular complex). Only intervesicular interaction is expected to induce aggregation, adhesion, or fusion of vesicles. Such ion recognition has been described in the clustering of vesicles, containing negatively charged terpyridine (terpy)-functionalized phospholipids, induced by addition of Fe^{2+} ions (27). It was also shown that the complexation of Cu^{2+} to vesicles incorporating a synthetic lipid bearing an iminodiacetic head group induced reorganization within the lipid bilayer (28), and at high lipid concentration related vesicles were found to form columnar structured lipid bilayer stacks (29).

We have recently studied the complexation of Eu^{3+} ions to vesicles containing amphiphilic ligands composed of a β-diketone function as head group, two hexadecyl chains as lipophilic anchors, and two hydrophilic tetra- or hexaethyleneoxy spacers (30). It gives rise to an intravesicular complex at the interface of the vesicles, which induces the transport of europium ion across the lipid bilayer.

We report here on the behavior of vesicles decorated with the lipoligands **Bn** (Scheme 1) containing 2,2′-bipyridine (bipy) as metal ion coordination group. We describe the synthesis of bipy derivatives **Bn** containing 4, 10, and 14 ethyleneoxy units as spacers (**B4**, **B10**, and **B14**) and their incorporation into phospholipid vesicles. The longer spacers may render a ligand embedded in a given vesicle more accessible to ligands embedded in another vesicle and facilitate their intervesicular complexation. Addition of transition metal ions to the **B10** or **B14** vesicles induces intervesicular complexation of the bipy units followed by morphological changes consistent with a fusion process leading to giant multilamellar vesicles (MLVs).

Abbreviations: bipy, 2,2′-bipyridine; MLV, multilamellar vesicle; LUV, large unilamellar vesicle; EPC, egg phosphatidylcholine; PEG, polyethylene glycol.

†Present address: Synthèse et ElectroSynthèse Organiques, Unité Mixte de Recherche 6510, Centre National de la Recherche Scientifique, Université de Rennes 1, Bâtiment 10A, 35064 Rennes Cedex, France.

**To whom correspondence should be addressed. E-mail: lehn@isis.u-strasbg.fr.

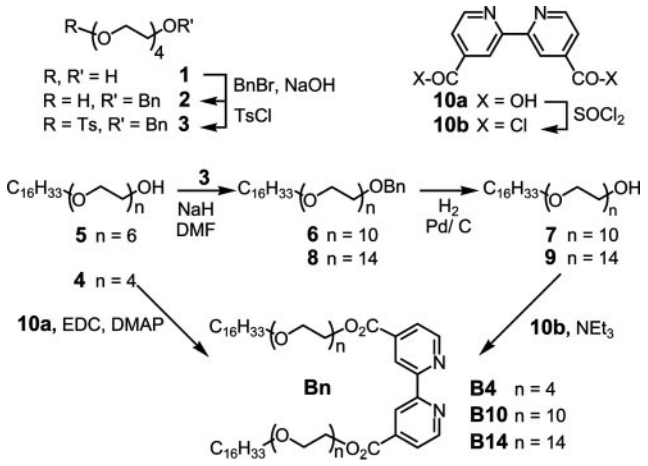

Scheme 1. Synthetic route for the preparation of the amphiphilic ligands **Bn**. BnBr, benzyl bromide; TsCl, tosyl chloride; DMF, dimethylformamide; EDC, *N*-ethyl-*N*′-(3-dimethylaminopropyl) carbodiimide hydrochloride; DMAP, 4-dimethylaminopyridine.

Methods

Synthesis of the bipy Ligands (Bn). ***General.*** Used for NMR ($CDCl_3$ solvent) was a Bruker AM200SY spectrometer equipped with an ASPECT 3000 data system; chemical shifts are reported in ppm downfield from tetramethylsilane; coupling constants, in Hz. Used for TLC was Merck silica gel 60 F254, 0.25 mm, UV or iodine vapor detection. Preparative column chromatography was done on a Merck silica gel 60 (0.040–0.063 mm) and aluminum oxide (0.063–0.200 nm) activity degree II-III. Elemental analyses were performed by Service Central d'Analyse du Centre National de la Recherche Scientifique, and differential scanning calorimetry was done on a Perkin–Elmer DSC7 instrument, with a heating or cooling rate of 5°/min unless otherwise stated; temperatures are reported in °C, and ΔH in kJ/mol.

Lipoligand B4. The 2,2′-bipyridine-4,4′-dicarboxylic acid **10a** (300 mg, 1.23 mmol, 1 eq) was dissolved in dimethylformamide (15 ml) under argon. The tetraethyleneglycol monohexadecyl ether **4** (1.25 g, 3 mmol, 2.5 eq), EDC (590 mg, 3 mmol, 2.5 eq), and DMAP (75 mg, 0.6 mmol, 0.5 eq) were added. The mixture was maintained at room temperature for 24 h under argon. After extraction with chloroform (30 ml) and washing with a NaCl solution, the organic phase was dried on Na_2SO_4. After evaporation of the solvent, the crude product was chromatographed [elution with a hexane/AcOEt gradient (30:70 to 20:80)] to provide **B4** (300 mg; yield, 24%). Melting point 50°C, ΔH = 130 kJ/mol. Mass spectroscopy for MH^+: 1045.8. NMR: ^1H ($CDCl_3$): 8.96 (s large, 2); 8.85 (d, 5.2 Hz, 2); 7.92 (dd, 5.2 Hz, 2); 4.55 (t, 5.2 Hz, 4); 3.87 (t, 5.2 Hz, 4); 3.69–3.57 (m, 68); 3.4 (t, 6.8 Hz, 4); 1.53 (t, 7 Hz, 4); 1.22 (s large, 56); 0.8 (m, 6).

Compound 2. Commercial tetraethyleneglycol **1** (58.50 g, 0.30 mol) and benzyl bromide (9.5 g, 0.055 mmol) were added to aqueous NaOH (50% wt/wt, 15 g, 0.38 mol). The reaction medium was refluxed for 24 h. After extraction with ether, the organic phase was washed with distilled water, dried over Na_2SO_4, and concentrated. The residue obtained (9.7 g) was chromatographed [silica gel 90 g, elution with ether and ether/MeOH (97:3)] to provide compound **2** (6.65 g, 43%). ^1H NMR ($CDCl_3$): 7.29 (m, 5); 4.52 (s, 2); 3.61 (m, 14); 3.12 (s, 2).

Compound 3. Tosyl chloride (4 g, 20.98 mmol) was added to a mixture of **2** (2.045 g, 7.04 mmol) and pyridine (1.62 ml, 21.11 mmol) in dry CH_2Cl_2 (20 ml) at 0°C. The reaction medium was maintained at 4°C for 48 h. After extraction with ether, the organic phase was washed three times with 5% (wt/wt) aqueous HCl, dried over Na_2SO_4, and concentrated. The crude product was chromatographed (silica gel 150 g, elution AcOEt gradient in CH_2Cl_2) to afford compound **3** (2.879 g, 93%). ^1H NMR ($CDCl_3$): 7.75 (d, 8 Hz, 2); 7.26 (m,7); 4.49 (s, 2); 4.08 (t, 5 Hz, 2); 3.60–3.51 (m, 14); 2.37 (s, 3).

Compound 6. To an ice-cooled solution of commercial hexaethyleneglycol monohexadecyl ether **5** (3.048 g, 6.015 mmol) in dry dimethylformamide (30 ml), was added NaH (60% suspension in oil, 602 mg, 15.038 mmol) with stirring. The reaction mixture was kept at 4°C for 30 min and then **3** (2.899 g, 6.617 mmol) was added. It was thereafter maintained at room temperature for 20 h. After hydrolysis with ice water, it was extracted with diethyl ether (80 ml), dried over Na_2SO_4, and concentrated. The residue (4.588 g) was chromatographed (silica gel 200 g, elution AcOEt/MeOH 90:10) to afford compound **6** (3.905 g, 84%). ^1H NMR ($CDCl_3$): 7.28–7.20 (m, 5); 4.49 (s, 2); 3.59–3.51 (m, 40); 3.37 (t, 7 Hz, 2); 1.5 (t, 6 Hz, 2); 1.18 (s, 28); 0.81 (t, 6 Hz).

Compound 7. A mixture of **6** (4.006 g, 5.182 mmol) and 10% Pd/C (500 mg) in absolute ethanol (50 ml) was stirred under hydrogen atmosphere for 2 h. After filtration, washing with ethanol, and evaporation under vacuum, the product was recrystallized in cold ethanol to afford compound **7** (1.772 g, 50%). ^1H NMR ($CDCl_3$): 3.59–3.51 (m, 40); 3.37 (t, 7 Hz, 2); 1.5 (t, 6 Hz, 2); 1.15 (s, 28); 0.79 (t, 6 Hz, 3).

Compound 8. Compound **8** was prepared by the same procedure described for **6**, from **7** (1 g, 1.46 mmol), NaH (60% in oil, 147 mg, 3.66 mmol), and **3** (0.706 g, 1.61 mmol). The crude product was chromatographed (silica gel 200 g, elution AcOEt/MeOH 85:15) and recrystallized twice in ethanol at 4°C to afford compound **8** (900 mg, 66%). ^1H NMR ($CDCl_3$): 7.28–7.22 (m, 5); 4.50 (s, 2); 3.57–3.50 (m, 54); 3.37 (t, 7 Hz, 2); 1.5 (t, 6 Hz, 2); 1.19 (s, 28); 0.81 (t, 6 Hz,3).

Compound 9. Compound **9** was prepared by the same procedure described for **7**, from **8** (900 mg, 0.963 mmol) and 10% Pd/C (100 mg). The crude product was recrystallized twice in ethanol at 4°C to afford compound **9** (600 mg, 73%). NMR: ^1H ($CDCl_3$): 3.61–3.53 (m, 58); 3.41 (t, 7 Hz, 2); 1.5 (t, 6 Hz, 2); 1.15 (s, 28); 0.84 (t, 6 Hz, 3).

Lipoligand B10. Commercial 2,2′-bipyridine-4,4′-dicarboxylic acid **10a** (100 mg, 0.41 mmol) was poured into thionyl chloride (8 ml) under argon. The reaction medium was refluxed for 24 h. After evaporation of the thionyl chloride, the crude acyl chloride **10b** in dry $CHCl_3$ (10 ml) was mixed with triethylamine (650 μl, 4.62 mmol) and **7** (620 mg, 0.91 mmol) was added. The mixture was maintained for 24 h under argon at room temperature. After washing with water (5 ml) and extraction with CH_2Cl_2, the organic phase was dried over Na_2SO_4 and concentrated. The residue was chromatographed (aluminum oxide 70 g, elution with toluene and toluene/acetone 50:50) and recrystallized three times in cold ethanol to afford compound **B10** (296 mg, 46%). Melting point 44.7°C, ΔH = 190 kJ/mol. Elemental analysis: calculated (%) for $C_{84}H_{152}N_2O_{24},H_2O$ (1574.10): C 63.37, H 9.75, N 1.76; found: C 63.13, H 9.67, N 1.61. NMR: ^1H ($CDCl_3$): 8.96 (s, 2); 8.85 (d, 5 Hz, 2); 7.91 (d, 5 Hz, 2); 4.55 (t, 5 Hz, 4); 3.87 (t, 5 Hz, 4); 3.69–3.57 (m, 68); 3.43 (t,7 Hz, 4); 1.56 (t, 7 Hz, 4); 1.24 (s, 56); 0.87 (t, 6 Hz, 6).

Lipoligand B14. **B14** was prepared by the same procedure described for **B10**, from **10a** (77 mg, 0.32 mmol), thionyl chloride (8 ml), and triethylamine (650 μl, 4.625 mmol) and **9** (0.6 g, 0.698 mmol). The crude product was chromatographed (aluminum oxide 80 g, elution with toluene/acetone 50:50 and toluene/acetone/MeOH 50:40:10) and recrystallized from cold ethanol to afford compound **B14** (380 mg, 62%). Melting point 44.0°C, ΔH = 221 kJ/mol. Elemental analysis: calculated (%) for $C_{100}H_{184}N_2O_{32}$ (1926.53): C 62.34, H 9.79, N 1.45; found: C 62.23, H 9.79, N 1.35. ^1H NMR ($CDCl_3$): 8.95 (s, 2); 8.84 (d, 4 Hz, 2; 7.90 (d, 4 Hz, 2); 4.54 (t, 5 Hz, 4);3.86 (t, 5 Hz, 5); 3.72–3.52 (m, 102); 3.43 (t, 7 Hz, 4); 1.56 (t, 7 Hz, 4); 1.24 (s, 56); 0.86 (t, 6 Hz, 6).

Vesicle Preparation and Characterization. ***Extrusion method.*** Large unilamellar vesicles (LUVs) were prepared by the extrusion method (31). A lipidic film was prepared from a mixture (97:3) of egg phosphatidylcholine (EPC; Sigma) and **Bn** (total 14 μmol) by evaporation of the organic solvent under reduced pressure. The film was then hydrated with a glucose solution (100 mM). After five freezing cycles in liquid nitrogen, the obtained suspension of MLVs was extruded through a polycarbonate filter with sized pores of 100 nm (Cyclopore Track Etchet Membrane, Whatman) 10 times with an extruder apparatus (Thermobarel Extruder, Lipex Biomembranes, Vancouver, BC, Canada) at 50°C. The resulting suspension of LUVs was filtered through an exclusion gel column (PD-10 columns, Sephadex G-25, Pharma Biotech). The final total lipid concentration of the 3 mol % **Bn** LUV suspension was 4.7 mM.

UV spectroscopy. UV measurements were carried out on a UV DU 640 spectrometer (Beckman) and fluorescence spectra were recorded on a SPEX Fluoromax spectrometer both at 20°C. Each 3 mol % **Bn** LUV suspension was titrated by the different isoosmolar solutions containing one of the following salts: $NiCl_2$, $CoCl_2$, $CaCl_2$, or NaCl.

Differential scanning calorimetry. The samples were prepared from a lipidic film of the desired lipid mixture (140 μmol) and hydrated with distilled water (500 μl), then heated, frozen, and vortexed until obtaining a homogenous opalescent suspension of MLVs. This suspension (50 mg) was introduced into a stainless steel pan and submitted to several cycles of cooling and heating at 5°C/min.

Dynamic light-scattering measurements. The vesicles were passed through filters (Nuclepore, pore size: 0.25 μm) at 0.1–0.5 mM lipid concentrations. The dynamic light-scattering measurements were carried out on a 4700/PCS/100 (Malvern Instruments, Malvern, U.K.) at several angles. A coherent argon laser at 514.5 nm produced incidence irradiation. Correlation functions were analyzed by the method of cumulants to give the hydrodynamic diameters.

Electron microscopy. To achieve the best preservation of the sample structure upon cryofracture, a water/33% (vol/vol) glycerol solution was used instead of a pure aqueous solution. A 20- to 30-mm-thick layer of the sample was deposited on a thin copper holder and then rapidly quenched in liquid propane. The frozen samples were fractured *in vacuo* ($\approx 10^{-7}$ torr) with a liquid nitrogen-cooled knife inside a Balzers 301 freeze-etching unit. The replication was done by using unidirectional shadowing with platinum-carbon at the angle of 35°. The mean thickness of the metal deposit was 1–1.5 nm. The replicas were washed with organic solvents and distilled water and then observed in a Philips EM 410 electron microscope. The contrast in images is related to the depth fluctuations of the metal deposit.

Optical microscopies. The 3 mol % **Bn** LUV sample was incubated in the presence of an isoosmolar solution of the desired salt completed with glucose to adjust the osmolarity. Samples were observed with an Olympus IX70 microscope equipped with a phase-contrast setup, dark-field condenser, and fluorescence. The images were recorded with a black and white Cohu video camera. To test the vesicle fusion, the 3 mol % **Bn** LUVs were prepared in the presence of the water-soluble chromophore rhodamine B (Sigma) at a concentration of 50 μM and filtered twice through an exclusion gel column (PD-10 columns, Sephadex G-25, Pharma Biotech) to remove the excess of rhodamine B from the external medium. The 3% mol **Bn** LUVs obtained were then incubated in presence of 5 mM $NiCl_2$. After several hours of incubation, the fusion process resulting in giant vesicles was followed by optical fluorescence, phase-contrast, and polarized light microscopies.

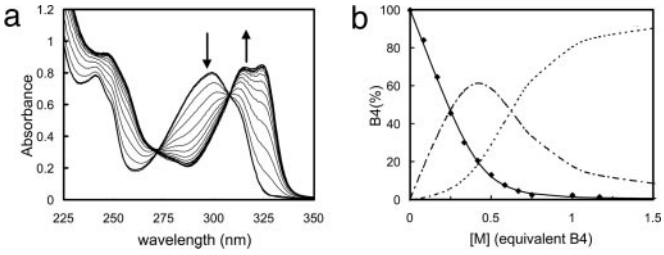

Fig. 1. Titration of a solution of lipoligand **B4** at 67.7 μM by $NiCl_2$ in ethanol. (*a*) Experimental UV spectra; the spectra of free ligand $A_L(\lambda)$ and complexed ligand $A_C(\lambda)$ are in bold; all spectra $A(\lambda)$ have been fitted by least-squares error minimization, supposing $A(\lambda) = x \cdot A_L(\lambda) + (1 - x) \cdot A_C(\lambda)$. (*b*) Calculated free ligand molar fraction x (◆); the data could be fitted only by assuming two successive complexation equilibria, M + **B4** ⇌ M**B4** and M**B4** + **B4** ⇌ M(**B4**)$_2$ with the formation constants log K_1 = 6.5 and log K_2 = 5.1; lines show calculated ligand molar fractions in **B4** (solid line), M**B4** (dotted line), and M(**B4**)$_2$ (dash-dot line).

Results and Discussion

Synthesis and Complexation Properties of the Lipoligands Bn in Solution. Amphiphilic ligands bearing two long hexadecyl chains, hydrophilic spacers of different lengths, and a bipyridine head group were prepared according to the route presented in Scheme 1. Tetraethyleneglycol was monobenzylated and then tosylated to give **3**. Compound **3** was condensed with the commercial ether **5** to give the compound **6**, which was deprotected to afford **7**. By following the same two-step procedure, compound **9** was obtained from **7** and **3**. Compound **B4** was obtained by condensation of 2,2′-bipyridine-4,4′-dicarboxylic acid **10a** with commercial tetraethyleneglycol monohexadecyl ether **4** in presence of DMAP and EDC. To improve the yield, the conditions were changed for the preparation of compounds **B10** and **B14**. The diacid **10a** was converted into the corresponding acid chloride **10b** and then condensed with alcohols **7** and **9** to give **B10** and **B14**, respectively.

In solution, complexation of the amphiphilic bipy compounds **Bn** by a metal ion M was followed by UV spectroscopy. With Ni^{2+}, the band at 300 nm attributed to the $\pi \rightarrow \pi^*$ transition of the bipy aromatic rings of the ligands **Bn** was shifted to higher wavelength at 324 nm in the complex (Fig. 1*a*). Titration of **Bn** by Ni^{2+} in ethanol is in good agreement with the formation of complexes M**Bn** and M**Bn**$_2$ with (1:1) and (1:2) stoichiometries as shown in Fig. 1*b* for **B4**. Note that the observed complex presents only two ligands **Bn** instead of three, as for the parent Ni(bipy)$_3$ complex (32).

Incorporation of the Lipoligands Bn into Vesicle Membranes. The incorporation of the amphiphiles **Bn** into an EPC bilayer membrane was investigated by differential scanning calorimetry measurements (see Table 1, which is published as supporting information on the PNAS web site). The amphiphiles present a peak corresponding to the fusion of the hexadecyl alkyl chains in pure thermotropic phase. The longer the polyethylene glycol (PEG) spacer, the more important is the decrease of the fusion temperature in the presence of water. Similarly, the fusion enthalpy decreases in the case of long spacers (**B10** and **B14**), whereas it is not significantly affected by the presence of water in the case of the shorter one (**B4**). Finally, on incorporation of a **Bn** ligand into an EPC MLV suspension, no fusion peak was observed, except in the case of **B4**, which appears to be at least partially segregated from the EPC so that the fusion of the compound **B4** was observed. The solubility of the **Bn** lipoligands in an EPC bilayer appears to increase with the spacer length, as expected from the size increase of the hydrophilic PEG head group.

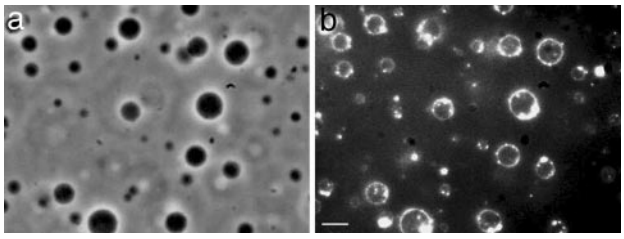

Fig. 2. Images of LUVs (100 nm at the beginning) containing 3 mol % lipoligand **B10** after an incubation time of 2 h in the presence of $NiCl_2$ (0.1 mM) obtained by phase-contrast optical microscopy (*a*) and dark-field optical microscopy (*b*). (Scale bar, 10 μm.)

Morphological Changes of Bn-Containing Vesicles Induced by Addition of Ni^{2+} and Co^{2+}: Vesicle Fusion. To investigate the effect of the addition of metal ions onto vesicles containing **Bn** lipoligands, the samples were observed by various complementary optical microscopy techniques. LUVs containing 3 mol % **B10** were first incubated in presence of Ni^{2+} and Co^{2+}. By optical phase-contrast microscopy one can observe very dark spherical objects of a diameter of several micrometers after an incubation time of 22 h (Fig. 2*a*). The same picture, observed by dark-field setup, exhibits bright circles corresponding to the scattering of the membrane of a vesicle (Fig. 2*b*). This latter technique allows confirmation of the presence of an inner aqueous compartment. Therefore, starting from LUVs of ≈100-nm diameter, the complexation with Ni^{2+} or Co^{2+} resulted in the formation of giant vesicles.

When studied by phase-contrast microscopy, the vesicles exhibited a strong contrast that may be considered to result from a large difference between the refractive indices of the external medium and the inner compartment that were initially identical. This observation may be attributed to the multilamellar character of the resulting giant vesicles.

To further investigate this phenomenon, the same samples were observed by polarized light optical microscopy and cryofracture electron microscopy. At first, the initial suspension of vesicles was essentially composed of unilamellar vesicles ≈100 nm in diameter prepared by extrusion (see Fig. 6, which is published as supporting information on the PNAS web site). After the same incubation time in the presence of Ni^{2+} ions, very large MLVs were observed (Fig. 3*a*), some of them being also multivesicular. Their morphology was similar to that of the so-called onion structure described in the literature (33). In a similar experiment with lipoligand **B14**, after 12 h of incubation, a giant vesicle resulting from multifusion events was observed by polarized light optical microscopy. As shown in Fig. 3*b*, it displayed Malta crosses corresponding to the texture defect of a lamellar phase. These findings indicate the formation of multilamellar stacking within the giant vesicle induced by the addition of Ni^{2+}.

These experiments reveal that the addition of Ni^{2+} or Co^{2+} ions to vesicles containing 3 mol % lipoligand **B10** or **B14** induces the formation of giant MLVs after a rather long incubation time (>1 h). One can envision two mechanisms for this fusion process. It may occur either by pore opening between the two compartments or by a membrane rupture resulting in the leakage of the aqueous compartments in the medium.

To elucidate the mechanism of the fusion process, the inner compartment of the LUVs containing 3 mol % **B14** was labeled with rhodaminedisulfonate, a fluorescent dye soluble in water. The dynamics of the fusion was followed in real time by video-enhanced optical phase-contrast and fluorescence microscopies. At first, the LUVs were incubated in the presence of Ni^{2+} until giant vesicles were observable. Many fusion events between these giant vesicles were seen to occur in about 10 s, as shown in

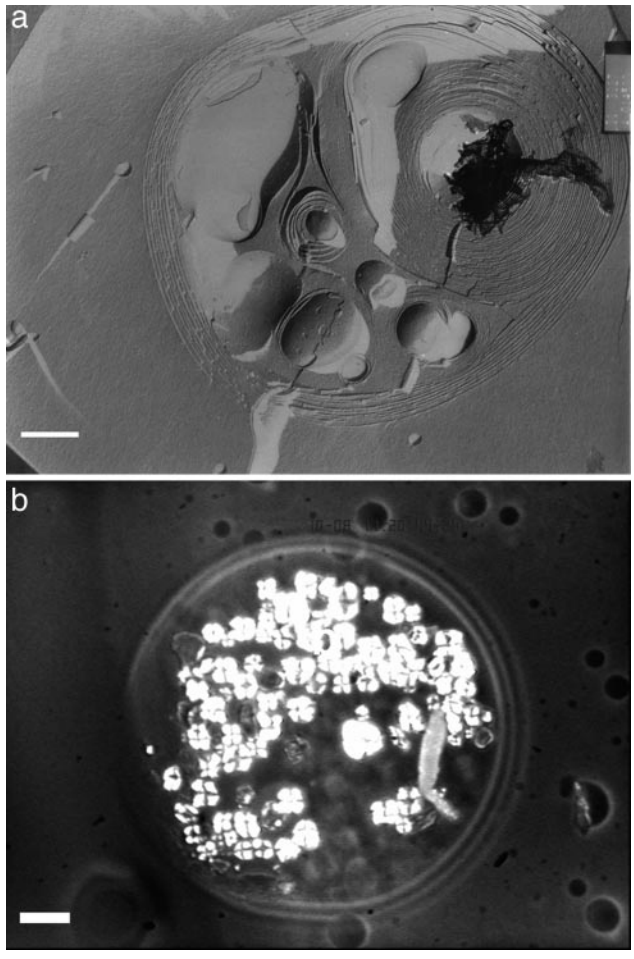

Fig. 3. Characterization of the MLVs generated by incubation of LUVs with $NiCl_2$. (*a*) Images of MLVs obtained by cryofracture electron microscopy after incubation of LUVs containing 3 mol % lipoligand **B10** for 24 h in the presence of $NiCl_2$ (0.1 mM). (Scale bar, 500 nm.) (*b*) Image of a giant vesicle resulting from the incubation of LUVs containing 3 mol % **B14** in the presence of $NiCl_2$ (0.1 mM) during 24 h observed by polarized light optical microscopy. (Scale bar, 10 μm.)

Movie 1, which is published as supporting information on the PNAS web site. Furthermore, these vesicles were strongly fluorescent, in contrast to the external medium, indicating that the rhodamine probe remained in the internal aqueous compartment of the vesicles. The fusion events could be followed by fluorescence microscopy, which gave clear images of the progressive merging of two vesicles into a single one (Fig. 4). Neither leakage of the fluorescent solution into the external medium nor decrease in the fluorescence intensity of the inner compartment of the vesicles was observed. In addition, the kinetics was very slow compared with a similar process recently reported for the fusion of unilamellar giant vesicles (<33 ms after the adhesion) (34), a result confirming that the vesicles resulting from multiple fusions are multilamellar.

Evidence for Metal Ion Complexation to the Vesicles. To elucidate the nature of the interaction and test the ability of the ligands **Bn** to complex metal ions at the interface of vesicles, the UV spectra of the vesicle suspension were recorded before and after addition of a solution containing divalent metal ions Ni^{2+} or Co^{2+}, which have octahedral coordination geometry. A control experiment was carried out with Ca^{2+} ions, which do not bind to bipy groups. The same experiment was performed for each amphiphile **Bn**.

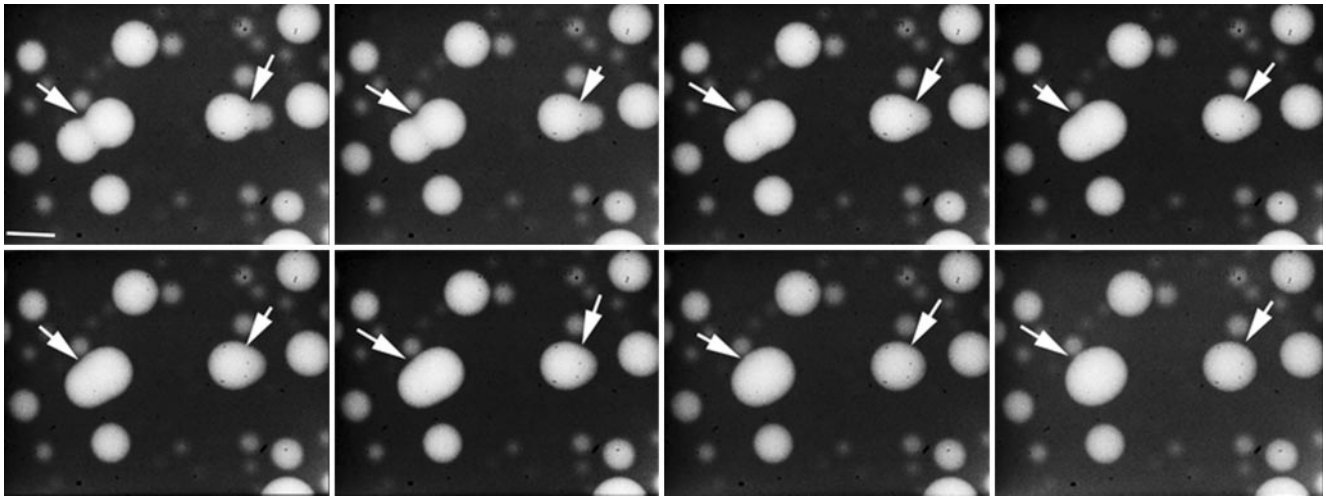

Fig. 4. Evolution in time of the generation of giant vesicles (arrows) resulting from the fusion of 3 mol % **B14** LUVs containing the rhodaminedisulfonate probe (50 μM) in the presence of $NiCl_2$ (0.1 μM) observed by optical fluorescence microscopy after an incubation time of 12 h. The time between the first picture (*Upper Left*) and the last one (*Lower Right*) was 7 s. (Scale bar, 10 μm.)

Whereas the addition of Ca^{2+} did not modify the UV spectrum of the vesicle suspension, the addition of the Ni^{2+} or Co^{2+} ions induced the appearance of an absorption band corresponding to the $M(\mathbf{Bn})_2$ complex with Ni^{2+} or Co^{2+} (at 325 nm) after 30 min as shown for **B14** in Fig. 7, which is published as supporting information on the PNAS web site. These results showed that the ligands **Bn**, incorporated in the membrane of EPC vesicles, formed a colored complex with Ni^{2+} or Co^{2+} in a relatively short time (<30 min) whatever the length of the PEG spacer.

In addition, the peak corresponding to the light scattering of 100-nm vesicles, observed below 300 nm, was not affected by the formation of the complex, which indicated that no significant change occurred in vesicle size. In **B10** and **B14**, after a long incubation time (22 h) a large increase of the turbidity of the solution was observed because of the fusion process, whereas no change was observed in **B4**.

Role of the Spacer Length of the Bn Lipoligand in the Fusion Process. Dynamic light-scattering experiments were performed for each **Bn** vesicle suspension in the absence or in the presence of various metal ions. The mean vesicle diameters obtained from these measurements are displayed in Fig. 5.

For a short PEG spacer as in **B4**, no change occurred in vesicle size even after several hours of incubation. In contrast, a large increase in the vesicle size was observed in the case of **B10** and **B14** possessing long spacers. The scattering objects were still growing after the end of the complexation step (<30 min). In the present system, the binding of metal ions to the bipy units results in an increase of the positive surfacic charge of the vesicle membrane and therefore in an electrostatic repulsion between vesicles. Moreover, neither complexation with bipy nor size increase was observed on addition of Ca^{2+} to **Bn** vesicles. Therefore, the formation of the metal ion complex observable by UV spectroscopy appears as the necessary first step to induce fusion between LUVs. In summary, the fusion process resulting in the formation of giant MLVs requires (*i*) a sufficiently long PEG spacer ($n = 10$ or 14) and (*ii*) the coordination of metal ions to the bipy head groups of **Bn** lipoligands belonging presumably to different vesicles.

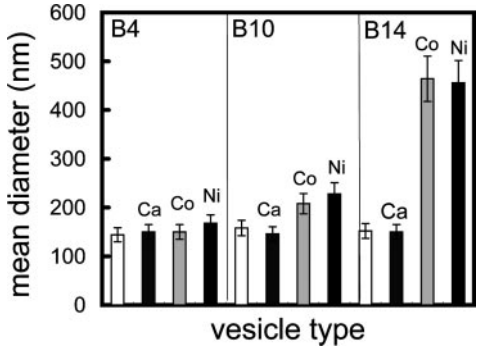

Fig. 5. Mean diameters of vesicles containing 3 mol % lipoligand **Bn** in the absence and after incubation in the presence of the metal ions Ca^{2+}, Co^{2+}, or Ni^{2+}, obtained by dynamic light scattering.

Evidence of a Critical Concentration of Bn Lipoligand in the Bilayer Membranes for Inducing Vesicle Fusion. To analyze the role of the **Bn** lipids in this process, similar dynamic light-scattering measurements were performed on vesicles containing various surface concentration of **B14** and **B10**. No fusion occurred in the vesicles containing 1 mol % **B14**, whereas fused vesicles were observed for 2 or 3 mol % **B14** (see Fig. 8, which is published as supporting information on the PNAS web site). The same experiment performed on vesicles containing different amounts of **B10** (1, 2, and 3 mol %) showed that fusion events occurred only for a concentration of 3 mol % **B10**. The threshold concentration appears to decrease as the spacer length increases. These experiments showed the existence of a critical concentration below which metal ion complexation without fusion was observed.

Discussion

On the basis of the data reported, the fusion events observed between vesicles containing the amphiphilic bipy derivatives, the lipoligands **Bn**, appear to depend on three parameters: (*i*) a minimal size of about 10 units for the PEG spacer; (*ii*) the nature of the complexing ion: only transition metal ions are able to initiate the fusion; and (*iii*) the existence of a threshold concentration under which only intravesicular complexation without fusion is observed. Furthermore, the initially unilamellar vesicles tend to undergo multilamellar stacking due to the formation of the bipy complexes between the bilayers. Such strong stacking of bilayers was previously observed in the complexation of Cu^{2+} by

an iminodiacetic lipid (29). It can be attributed here to the strong affinity of Ni^{2+} or Co^{2+} ions for the bipy coordination group.

Two different kinetics were observed for the complexation and the fusion processes. The complexation at the interface, whatever the length of the spacer, was completed in <30 min and therefore does act as the first step. In contrast, the fusion process takes place over several hours after the ion complexation onto the membrane. In agreement with all the experimental results, the following mechanism can be proposed: (*i*) formation of intravesicular complexes M**Bn** and M(**Bn**)$_2$; (*ii*) ligand exchange with formation of intervesicular complexes between ligands belonging to different vesicles in the case of a long PEG spacer; (*iii*) reinforcement of the attachment between the two adjacent membranes; (*iv*) strong adhesion with multilayer formation; and (*v*) fusion by pore opening between the two aqueous compartments of the vesicles. The formation of an intervesicular complex is made possible by the presence of a sufficiently long PEG spacer that allows the ligands embedded in one vesicle bilayer to reach over to the complexes formed of the surface of a different vesicle. The presence of a long spacer increases the probability to find a free ligand in a extended conformation as reported in the adhesive biotin–streptavidin system composed of ligands attached to a flexible tethered PEG polymer (35).

The question arises why the intervesicular complexation was followed by an irreversible fusion without leakage of the inner compartments and resulted in the formation of MLVs after many fusion events. The fusion between vesicles without leakage or rupture occurs by the formation of an unstable pore (36). The pore size is limited by its line tension energy cost, $\lambda \cdot 2\pi \cdot R$. Generally, this cost is not counterbalanced and the pore is spontaneously closed. In the present system, the formation of multilayers may be driven by metal ion selective binding with a surface energy gain γ. The surface excess generated by the pore is assumed to be involved in multilayer formation with an energy gain of $\gamma \cdot \pi \cdot R^2$. Thus, the formation energy of an intermediate pore, $E = \lambda \cdot 2\pi \cdot R - \gamma \cdot \pi \cdot R^2$ is decreasing when its radius is superior to a critical radius $R_c = \lambda/\gamma$. In this case, the pore size is not limited and the pore can increase indefinitely. In the same way, the large membrane excess resulting from fusion at constant volume and constant surface is involved in the formation of multilayers at the surface (Fig. 3*b*) with an energy gain resulting from the metal-ion binding.

To stabilize the adhesion state and the multilayer stacking, a minimal surface concentration of **Bn** within the membrane was required (3 mol % for **B10** and 2 mol % for **B14**). This observation indicates that the formation of a minimum number of intervesicular complexes at the junction is required to counterbalance the repulsion between the two membranes. The corresponding threshold concentration is expected to decrease with an increase of the length of the PEG spacer and a parallel increase in the number of intervesicular complexes that results in the reinforcement of the adhesion and the fusion processes.

Conclusion

The results described here indicate that vesicles incorporating lipidic ligands in their bilayer membrane may undergo various intervesicular processes (adhesion, fusion, etc.) induced by metal-ion binding, eventually extending to metal-ion-triggered drug and gene delivery by vesicle–cell interaction (37).

Such systems provide an attractive approach to the generation by self-assembly of structurally organized and functionally integrated multivesicular arrays (38) under the control of metallosupramolecular ligand/metal-ion recognition events. They open further perspectives toward the evolution of chemical systems of increasing complexity (7).

We thank Hubert Hervet for helpful discussions concerning the light-scattering measurements and Jean-Claude Dedieu for his assistance with the electron microscopy measurements.

1. Stanley, E. F. (1997) *Trends Neurosci.* **20,** 404–409.
2. Ahlers, M., Müller, W., Reichert, A., Ringsdorf, H. & Venzmer, J. (1990) *Angew. Chem. Int. Ed. Engl.* **29,** 1269–1285.
3. Ringsdorf, H. (2000) in *Physical Chemistry of Biological Interfaces*, eds. Baszkin, A. & Norde, W. (Dekker, New York), pp. 243–282.
4. Menger, F. M. & Gabrielson, K. D. (1995) *Angew. Chem. Int. Ed. Engl.* **34**, 2091–2106.
5. Paleos, C. & Tsiourvas, D. (2003) *Top. Curr. Chem.* **227,** 1–29.
6. Antonietti, M. & Förster, S. (2003) *Adv. Mat.* **15,** 1323–1333.
7. Lehn, J.-M. (2002) *Proc. Natl. Acad. Sci. USA* **99,** 4763–4768.
8. Shimomura, M., Nakamura, F., Ijiro, K., Taketsuna, H., Tanaka, M., Nakamura, H. & Hasebe, K. (1997) *J. Am. Chem. Soc.* **119,** 2341–2342.
9. Berti, D., Baglioni, P., Bonaccio, S., Barsacchi-Bo, G. & Luisi, P. L. (1998) *J. Phys. Chem. B* **102,** 303–308.
10. Thibault, R. J., Jr., Galow, T. H., Turnberg, E. J., Gray, M., Hotchkiss, P. J. & Rotello, V. M. (2002) *J. Am. Chem. Soc.* **124,** 15249–15254.
11. Tareste, D., Pincet, F., Perez, E., Rickling, S., Mioskowski, C. & Lebeau, L. (2002) *Biophys. J.* **83,** 3675–3681.
12. Pincet, F., Lebeau, L. & Cribier, S. (2001) *Eur. Biophys. J.* **30,** 91–97.
13. Shohda, K.-I., Toyota, T., Yomo, T. & Sugawara, T. (2003) *ChemBioChem* **4,** 778–781.
14. Yoshina-Ishii, C. & Boxer, S. G. (2003) *J. Am. Chem. Soc.* **125,** 3696–3697.
15. Kersey, F. R., Lee, G., Marszalek, P. & Craig, S. L. (2004) *J. Am. Chem. Soc.* **126,** 3038–3039.
16. Lehn, J.-M. (2002) *Polym. Int.* **51,** 825–839.
17. Marchi-Artzner, V., Jullien, L., Gulik-Krzywicki, T. & Lehn, J.-M. (1997) *Chem. Commun.*, 117–118.
18. Marchi-Artzner, V., Gulik-Krzywicki, T., Guedeau-Boudeville, M.-A., Gosse, C., Sanderson, J. M., Dedieu, J.-C. & Lehn, J.-M. (2001) *ChemPhysChem* **2,** 367–376.
19. Marchi-Artzner, V., Lehn, J.-M. & Kunitake, T. (1998) *Langmuir* **14,** 6470–6478.
20. Marchi-Artzner, V., Artzner, F., Karthaus, O., Shimomura, M., Ariga, K., Kunitake, T. & Lehn, J.-M. (1998) *Langmuir* **14,** 5164–5171.
21. Lehn, J.-M. (1995) *Supramolecular Chemistry: Concepts and Perspectives* (VCH, Weinheim, Germany), pp. 139–197.
22. Atwood, J. L., Davies, J. E. D., MacNicol, D. D., Vögtle, F. & Lehn, J.-M., eds. (1996) *Comprehensive Supramolecular Chemistry* (Pergamon, Oxford), Vol. 9.
23. Swiegers, G. F. & Malefetse, T. J. (2000) *Chem. Rev. (Washington, DC)* **100**, 3483–3537.
24. Leininger, S., Olenyuk, B. & Stang, P. J. (2000) *Chem. Rev. (Washington, DC)* **100,** 853–908.
25. Simon, J., Le Moigne, J., Markovitsi, D. & Dayantis, J. (1980) *J. Am. Chem. Soc.* **102,** 7247–7252.
26. Le Moigne, J. & Simon, J. (1980) *J. Phys. Chem.* **84,** 170–177.
27. Constable, E. C., Meier, W., Nardin, C. & Mundwiler, S. (1999) *Chem. Commun.*, 1483–1484.
28. Sasaki, D. Y., Shnek, D. R., Pack, D. W. & Arnold, F. H. (1995) *Angew. Chem. Int. Ed. Engl.* **34,** 905–907.
29. Waggoner, T. A., Last, J. A., Kotula, P. G. & Sasaki, D. Y. (2001) *J. Am. Chem. Soc.* **123,** 496–497.
30. Marchi-Artzner, V., Brienne, M.-J., Gulik-Krzywicki, T., Dedieu, J.-C. & Lehn, J.-M. (2004) *Chem. Eur. J.*, 2342–2350.
31. Olson, F., Hunt, C. A., Szoka, F. C., Vail, W. J. & Papahadjopoulos, D. (1979) *Biochim. Biophys. Acta* **557,** 9–23.
32. Mason, S. F., Peart, B. J. & Waddell, R. E. (1973) *J. Chem. Soc. Dalton Trans.*, 944–949.
33. Diat, O., Roux, D. & Nallet, F. (1993) *J. Phys. II France* **3,** 1427–1452.
34. Nomura, F., Inaba, T., Ishikawa, S., Nagata, M., Takahashi, S. & Hirokazu, H. (2004) *Proc. Natl. Acad. Sci. USA* **101,** 3420–3425.
35. Jeppesen, C., Wong, J. Y., Kuhl, T. L., Israelachvili, J. N., Mullah, N., Zalipsky, S. & Marques, C. M. (2001) *Science* **293,** 465–468.
36. Karatekin, E., Sandre, O., Guitouni, H., Borghi, N., Puech, P.-H. & Brochard-Wyard, F. (2003) *Biophys. J.* **84,** 1734–1749.
37. Guo, X. & Szoka, F. C., Jr. (2003) *Acc. Chem. Res.* **36,** 335–341.
38. Stamou, D., Duschl, C., Delamarche, E. & Vogel, H. (2003) *Angew. Chem. Int. Ed. Engl.* **42,** 5580–5583.